Zhuang, X., Ourselin, S., Razavi, R., Hill, D. L. G, Hawkes, D. J. (2008). Automatic Whole Heart Segmentation Based on Atlas Propagation with a Priori Anatomical Information. In Proc. Medical Image Understanding and Analysis 2008, Eds: S. McKenna and J. Hoey, pp. 29-33

Automatic Whole Heart Segmentation Based on Atlas Propagation with A Priori Anatomical Information

X. Zhuang [a*], S. Ourselin [a], R. Razavi [b], D. L. G. Hill [a], and D. J. Hawkes [a]

[a] Centre for Medical Image Computing, University College London, UK, WC1E 6BT;
[b] Interdisciplinary Medical Imaging Group, St Thomas' Hospital, KCL, UK, SE1 7EH

We propose a framework for automatic whole heart segmentation from cardiac MRI images based on atlas propagation. Firstly, we employ a new initialisation method incorporating anatomical constraints using region based registrations. Then, we apply a force-mask fluid registration to refine the registration between the atlas and the MRI image. Finally, we use a boundary searching method to fine-tune the segmented surface. In this framework, the impact of automating the segmentation propagation across populations has been improved due to the incorporation of the *a priori* anatomical information in the registration. In the experiments, we employed eight pathological data to evaluate the performance of the segmentation framework. The results show an average segmentation error of 1.7 ± 0.2mm.

1 Introduction

Cardiac MRI (CMRI) is one of the most important imaging modalities for investigating cardiac anatomy and pathophysiology in clinical applications. Accurate functional analysis from CMRI images needs accurate and unbiased segmentations. However, whole heart segmentation is currently challenging due to the image noise and artefacts, low tissue contrast, and the indistinct boundary information between the cardiac atria and major vessels. Currently, manual segmentation is one of the most reliable methods in clinical applications; however the segmentation results are subjective to inter- and intra-observer errors.

Two categories of techniques have shown the potentials of fully automatic segmentation from CMRI images.

The first category is based on segmentation propagation using registration techniques. These methods propagate the label information in a pre-constructed heart atlas to the MRI images for automatic segmentation [2, 3]. In these works, they employ a global affine registration to initialise the atlas and a non-rigid registration with a large number of degree of freedom (DOF) to fine-tune the detail. The initialisation with a single global affine transformation does not take any *a priori* anatomical information from the atlas or MRI image. This addresses a challenge for the non-rigid registration when the atlas and the MRI image have significant heart shapes, for instance when it comes to different pathological data. Therefore, the major disadvantage of these methods is that every single heart atlas can only be applied to a small number of specific images whose heart shapes are similar to that of the atlas.

The second category is based on a statistical model which builds the prior heart shape knowledge into the model to constrain the shape variations, e.g. [1]. By varying the value of the modes from the principle component analysis result, the statistical model can provide a large variation of heart shapes to initialise itself for MRI images from different subjects. The major challenge of these methods is the construction of the statistical model. Firstly, it needs a large number of training data which have already been segmented and whose heart shapes are representative of all possible image data. This representativeness is practically more challenging than the application itself. Secondly, most of the methods from this category incorporate image texture information into the model for boundary searching. This makes the segmentation tools vulnerable to the changeable parameters of the MRI sequences. Finally, some techniques such as [1] introduce more degree of freedom (DOF) into the model for local adaptation. This local adaptation which is based on image gradient makes the method sensitive to false boundaries caused from artefacts.

In this paper, we propose a framework for automatic whole heart segmentation from CMRI images based on atlas propagation using registration techniques with *a priori* anatomical information and a boundary detection. The method embeds the anatomical information from the atlas into the initialisation registration and the fluid registration to constrain the morphological correspondence and registration optimisation. The boundary correction employs multi-Canny edge images which maintain the boundary with low gradient to fine-tune the segmentation.

This paper is organised as follow. In section 2, we describe the methodology. In section 3, we evaluate the performance of the segmentation and different registration techniques using eight clinical data. Conclusion and discussion are given in section 4.

* Email: x.zhuang@ucl.ac.uk

2 Methodology

In this work, three steps are included for the whole heart segmentation. Firstly, the anatomical regions of the atlas are extracted to register to the corresponding regions in the MRI images to give a local misalignment-free starting estimate. Then, a force-mask fluid registration is employed to refine the label propagation. Both of these two steps embed the anatomical priors in the registration algorithms and use normalised mutual information similarity measure [11] because of the different intensity modalities of the atlas and CMRI images. Finally, a set of edge images computed from the standard Canny edge detection algorithm [7] but on three dimensional (3D) space are used to fine-tune the segmentation. Section 2.1 to 2.3 gives the detail of the three steps and Figure 2. shows the flowchart of the framework.

2.1 Anatomical constraints in the initialisation using region based registrations (IRBReg)

In our previous contribution [4], we proposed an initialisation method using region based registrations for two ventricle segmentations. In this paper, we extend this work to the whole heart segmentation. Figure 3 shows an atlas built from a healthy heart and a pathological heart MRI image. They are with large difference in terms of heart shapes. In Figure 1, we show the registration/ segmentation results between these two images. Figure 1 (a) shows the local misalignments based on a global affine transformation. This local misalignments lead to the failure of a fluid non-rigid registration between them as shown in Figure 1 (c): the non-blood tissue between the left atrium and the aorta is too thin for the registration algorithm to correct the misalignment. So is the boundary between the right atrium and the aorta. Therefore, we introduce the anatomical priors into the initialisation using region based registrations between each anatomical region to constrain the local alignment between the atlas and the CMRI image.

For the whole heart segmentation, the ventricles, atria, aorta, and pulmonary artery are all extracted from the atlas as independent images and separately aligned to the CMRI images using affine registrations to derive local transformations for each region. A revised distance weighting interpolation method proposed by Little *et al.* in [6] is used to generate a global deformation field from the local transformation set. Let $\{G_i\}$ be the set of local transformations assigned to each local region images, the global transformation fields T interpolated from this set can be expressed as:

$$T(X)=\begin{cases} G_i(X), & X \in V_i',\ i=1...n \\ f(X), & X \notin \bigcup_{i=1}^{n} V_i' \end{cases}, \tag{1}$$

where, V'_i represents the volumes which are the extracted local region V_i minus a volume which overlaps other local region V_k after their respective transformation G_i and G_k:

$$V_i' = V_i - (\bigcup_{i \neq k} \oplus_l R_{ik}) \ , \tag{2}$$

where, $R_{ik}=G_i^{-1}(G_i(V_i) \cap G_k(V_k))$; $\oplus_l$ is the morphology dilation with length l which is the minimal distance between each of the local regions. Therefore, there is no overlap between V'_i (more detail explanation *c.f.* [4]); and eq. (1) produces a smooth deformation field after the interpolation *f(x)* using a distance weighting function [5, 6]:

$$f(X) = \sum_{i=1}^{n+8} w_i(X) \times G_i(X) \ , \tag{3}$$

where, G_{n+1}, …, G_{n+8} are identity transforms for the eight vertex points of the cubic region of interest (ROI); and w_i is the inverse distance weighing function:

$$w_i(X) = \frac{1/d_i(X)^e}{\sum_{i=1}^{n+8} 1/d_i(X)^e} \ , \tag{4}$$

where, d is the Euclidean distance between point X and V_i based on the distance transformation algorithm [8]; d_{n+1}, …, d_{n+8} are the distance between the X to the ROI vertex points; the smoothness of interpolated deformation is determined by the choice of e (e>1 guarantees the first derivative is continuous). A value of 1.5 which was proposed in [6] is used in the experiments in section 3.

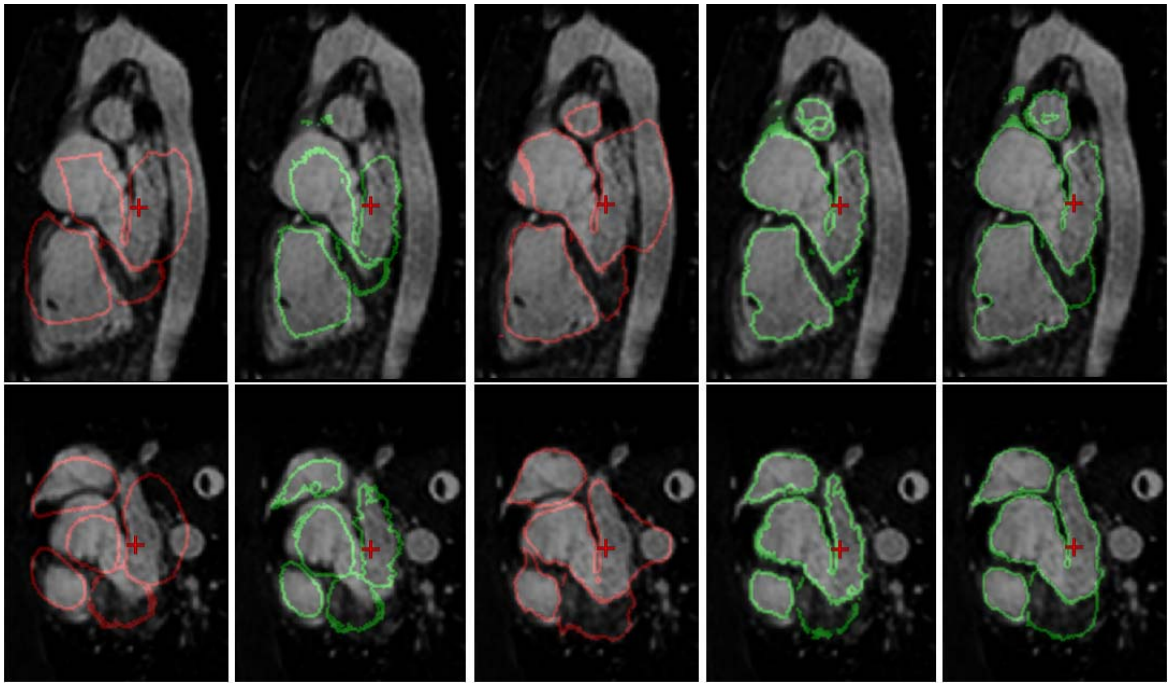

(a) (b) (c) (d) (e)

Figure 1. Demonstration of the performance of different registrations, we only focus on sagittal and axial views. The lines overlapped with the MRI image are contours of the atlas. Top row are sagittal view images, bottom row are axial view images. (a) shows the local misalignment after an affine registration; (b) shows the result after the initialisation using region based registration (IRBReg). (c) shows the result after a fluid registration based on the affine initialisation in (a). (d) shows the result after the force-mask fluid registration based on IRBReg in (b). (e) shows the segmentation result based on the proposed segmentation framework.

2.2 Incorporate anatomical priors within fluid registration

For the non-rigid registration, we choose to use fluid registration because the topology preservation is easily guaranteed by the physical property of a fluid model [9, 10]. In heart image registration, we have the prior knowledge that the shape of the heart blood region has much larger variation than the myocardial thickness has. Hence, in inter-subject registrations, the deformation model for aligning the blood pool needs more DOF and optimisation steps compared to that of the myocardium. Based on this knowledge, we use a blood region mask image for the fluid registration to compute the driving force:

$$Force(X) = \begin{cases} \nabla C(X), & X \in V_{blood} \\ 0, & X \notin V_{blood} \end{cases}, \tag{6}$$

where, C is the cost function. The driving force is only computed within the blood pool of the atlas. This not only saves more than 80% run-time for computing the fluid force, but also practically helps to decrease the possibility of registering the myocardium of the atlas to the papillary muscle of the CMRI image.

2.3 Multi-Canny edge images correction

In 3D isotropic CMRI images, the boundary between the epicardial surface and the liver tissue is indistinct; so is the boundary between the atria and major vessels. Therefore, instead of only using local gradient information for local adaptation, we propose to search closest Canny edge [7] for further local adaptation. There are three advantages this. Firstly, computing the Canny edge is much faster compared to a non-rigid registration. Secondly, the Hysteresis step in Canny edge computation preserves the global boundary connectivity information to protect the low gradient edges. Finally, only searching the closest Canny edges within a limit range from the resultant surface from the previous fluid registration step can help to avoid false edges from the artefacts. This is based on the assumption that the previous segmentation from the fluid registration is close enough to the ground truth. Practically, we use two threshold sets to compute the endocardial surface (threshold 0.2, 0.6), and the left ventricle epicardial surface (threshold 0.05, 0.2) for whole heart segmentation. Based on the segmented surfaces S from the fluid registration, we search the closest Canny edge points within 5mm to S to further correct it. The resultant S is two point-cloud

	0-2mm(%)	2-5mm(%)	>5mm(%)	SD(mm)	VO(%)
Left Ventricle	71 / ***72***	19 / ***20***	9.6 / ***8.2***	1.5 / ***1.7***	76 / ***77***
Right Ventricle	75 / ***77***	18 / ***16***	7.0 / ***7.1***	1.4 / ***1.6***	74 / ***76***
Epicardial Surface	66 / ***64***	23 / ***21***	10 / ***14***	1.8 / ***2.4***	53 / ***49***
Left Atrium	63 / ***42***	23 / ***18***	14 / ***40***	2.0 / ***7.2***	57 / ***40***
Right Atrium	71 / ***70***	17 / ***15***	12 / ***15***	1.8 / ***2.7***	70 / ***66***
Pulmonary artery	51 / ***54***	17 / ***16***	32 / ***30***	3.8 / ***4.8***	46 / ***44***
Aorta	85 / ***61***	11 / ***13***	3.8 / ***26***	1.1 / ***4.0***	61 / ***46***
Mean/ Standard deviation	68 ± 5.4 / ***65*** ± ***14***	20 ± 3.1 / ***18*** ± ***2.5***	10 ± 2.7 / ***17*** ± ***13***	1.7 ± 0.2 / ***3.1*** ± ***2.3***	66 ± 10 / ***61*** ± ***17***

Table 1. The quantitative evaluation of the performances of the proposed segmentation method with the initialisation using region based registration (IRBReg) (left to the slash), and the method based on fluid registration with a single affine registration initialisation (italic bold fond, right side of the slash). The segmentation errors are based on the surface distance (SD) and VO is the volume overlap [12] against the manual segmentations. Except the *Epicardial Surface* row whose VO is computing the left ventricle myocardium volume and its epicardial surface, all the others are computing the blood pool and the endocardial surface. The last row gives the mean value and standard deviation on the four chambers.

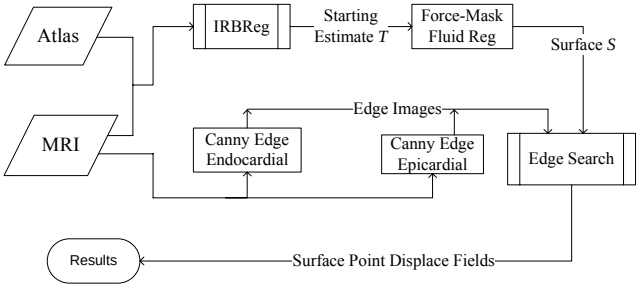

Figure 2. The flowchart of the proposed segmentation framework.

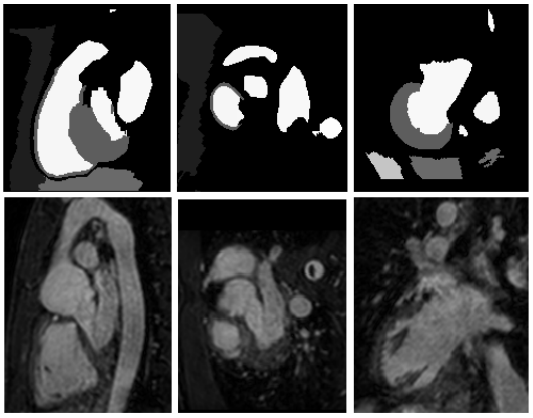

Figure 3. The three views of the atlas used in this work (top) and the MRI image (bottom) used in Figure 1: sagittal view (left), axial view (middle), and coronal view (right).

surfaces (endocardial and epicardial surfaces) based on which we can also construct mesh surfaces if they are desired.

3 Results

Eight patient data that have either dilated right ventricles or myocardium infarction are employed to test the performance of the proposed method. The MRI sequence is the balanced steady state free precession (b-SSFP) for whole heart imaging with acquisition resolution 2 × 2 × 2 mm and reconstruct into 1 × 1 × 1 mm. All the 8 data have been segmented using a semi-automatic tool provided from Philips. The automation of this tool is based on [1] and the manual correction is done by manually adapting the heart mesh to visually best segment the MRI images. The atlas used was built from a healthy volunteer with different regions labelled with different intensity values, as shown in Figure 3.

Figure 1 shows registration/ segmentation results of using different registration techniques: a single global affine registration (a), initialisation using region based registration (IRBReg) (b), a fluid registration with the initialisation using a single affine registration (c), a force-mask fluid registration with the IRBReg (d), and the segmentation result by the proposed segmentation framework. (We only give the sagittal and axial views on the atria and major vessel regions because the ventricle segmentations have been done in our previous work in [4]). In this example, the IRBReg shows the advantage over a single global affine registration in locally aligning the atria regions, which is important for the next-step non-rigid registration.

Table 1 shows the quantitative segmentation results of the proposed method and that of the fluid registration using a single global affine registration for initialisation. The surface distance, computed from the distance of a surface point in one image to the triangle plane formed by closest three surface points in the other image, and the volume overlap $((A \cap B)/(A \cup B))$ [12] between the resultant segmentations and the ground truth from the manual segmentations are calculated for each anatomical region. Although the ventricle segmentation shows no significant improvement by the proposed method compared to the results from the method using the fluid registration with a single affine initialisation, the segmentation on the atria and major vessels has shown a significant improvement.

4 Conclusion and discussion

In this paper, we propose a new framework for automatic whole heart segmentations from cardiac MRI images. The segmentation method benefits from the a *priori* anatomical information incorporated into the initialisation using region based registration (IRBReg) and the fluid registration. Furthermore, the Canny edge correction fine-tunes the label propagation from the atlas to the MRI images to achieve subvoxel accuracy. The results on eight pathological datasets have shown that the algorithm performs with an average 1.7 ± 0.2 mm surface distance, and 0.66 ± 0.10 volume overlap against the manual segmentation. This compares with an average surface distance 3.1 ± 2.3 mm, and volume overlap 0.61 ± 0.17 by using a fluid registration initialised with a single affine transformation. Special attention needs to be paid to the improvement in the segmentation of the cardiac atria and major vessels (shown in Table 1) which are the most challenging regions in the whole heart segmentation.

One limitation of this work is the heart localisation which determines the performance of the region based registration. In this work, we localise the heart using an affine registration. However some alternative methods will be considered in our future work, such as the method introduced in [1]. Another limitation is that the local regions are registered separately instead of competitively to the MRI image. This separation can lose their original geometrical relations and increase the probability of failing the initialisation. Future work includes improving the two limitations and applying the method to the segmentation on multi-frame or multi-time point data.

Acknowledgement

This work was funded by EPSRC grant GR/T11395/01. The authors would like to Dr. Kawal Rhode for help on the manual segmentation tool.

Reference

1. J. Peters, O. Ecabert, C. Meyer, H. Schramm, R. Kneser, A. Groth, and J. Weese, “Automatic Whole Heart Segmentation in Static Magnetic Resonance Image Volumes,” In Proc. MICCAI, 2007.
2. M. Lorenzo-Valdes, G. I. Sanchez-Ortiz, R. Mohiaddin, D. Rueckert, “Atlas-based segmentation and tracking of 3D cardiac MR images using non-rigid registration,” In Proc. MICCAI, pp. 642-650, 20024.
3. D. Perperidis, R. Mohiaddin, D. Rueckert, “Construction of a 4D statistical atlas of the cardiac anatomy and its use in classification,” In Proc. MICCAI, pp, 402-410, 2005.
4. X. Zhuang, D. J. Hawkes, W. R. Crum, R. Boubertakh, S. Uribe, D. Atkinson, P. Batchelor, T. Schaeffter, R. Razavi, D. L. G. Hill, “Robust registration between cardiac MRI images and atlas for segmentation propagation,” In Proc, SPEI on Medical Imaging, 2007.
5. D. Shepard, “A two-dimensional interpolation function for irregularly-spaced data,” In Proc, 23rd national Conference of the ACM, ACM Press, pp. 517-527, 1968.
6. J. A. Little, D. L. G. Hill, D. J. Hawkes, “Deformation incorporating rigid structures,” Computer Vision and Image Understanding, 66(2), pp. 223-232, 1997.
7. J. Canny, “A Computational Approach to Edge Detection,” IEEE Trans. Pattern Analysis and Machine Intelligence, vol. 8, no. 6, pp. 679-698, 1986.
8. T. Saito and J.I. Toriwaki, “New algorithms for Euclidean distance transformations of an n-dimensional digitised picture with applications,” Pattern Recognition, 27(11), pp. 1551-1565, 1994.
9. W. R. Crum, D. L.G. Hill, D. J. Hawkes, “Information theoretic similarity measures in non-rigid registration,” in Proc. IPMI 2003, LNCS 2732, pp. 378–387, 2003.
10. W. R. Crum, C. Tanner, D. J. Hawkes, “Anisotropic multi-scale fluid registration: evaluation in magnetic resonance breast imaging,” Phys. Med. Biol. 50(031-9155 (Print), 21), 5153-5174. ISSN: 0031-9155, 2005.
11. C. Studholme, D.L.G. Hill, D.J. Hawkes, “An overlap invariant entropy measure of 3D medical image alignment,” Pattern Recognition 32, pp. 71-86, 1999.
12. W. R. Crum, O. Camara, D. L. G. Hill, “Generalized overlap measures for evaluation and validation in medical image analysis,” IEEE Trans Med Imag, 25(11), pp. 1451-1461 2006.